arXiv:cond-mat/0101227v4 [cond-mat.mes-hall] 28 Aug 2002

Quantum wires and dots driven by intense surface acoustic waves and the quantum attenuation of sound in an electron plasma

A. O. Govorov*, A. V. Kalameitsev**, and V. M. Kovalev
Institute of Semiconductor Physics, Russian Academy of Sciences, Siberian Branch, 630090 Novosibirsk, Russia

Abstract

We develop a quantum theory of the nonlinear interaction between intense surface acoustic waves and electrons of a quantum well in the regime of moving quantum wires and dots. The quantum nonlinear interaction qualitatively differs from the classical one. In a system of electron wires driven by an acoustic wave the sound attenuation strongly decreases with increasing the sound intensity. However, even in the quantum limit the sound attenuation in the electron system remains nonzero due to residual scattering by impurities in the lowest subband. In the case of electron dots formed by two waves moving in the perpendicular directions, the calculated dissipation vanishes at high sound intensity because of the fully quantized spectrum. Besides, moving quantum dots can be formed by a single acoustic wave propagating along a system of etched quantum wires. We show that the quantum regime of the attenuation can exist in high-mobility GaAs quantum wells where the heating can not destroy the quantum state.

Typeset using REVTEX

I. INTRODUCTION

Quantum wires, channels, and dots are very intriguing objects in the modern solid-state physics. They display new physical properties due to reduced dimensionality. The electric conductance of narrow channels in a semiconductor nanostructures demonstrates the quantization [1] described by the Landauer-Büttiker theory [2]. More recently the quantized conductance has also been found for the thermal transport in free-standing quantum wires [3]. Furthermore the quantum wires and dots are attracting significant theoretical interest due to the enhanced many-particle interactions [4–6].

Experimentally, semiconductor quantum wires and channels are realized or by the electrostatic method or in etched nanostructures [1,7]. Recently, another method to create electron wires has been demonstrated [8,9]. This method involves an intense surface acoustic wave (SAW) in a hybrid structure [8] containing a semiconductor quantum-well and a strongly piezoelectric (PE) host crystal (Fig. 1a). In the experiments [8] a formerly homogeneous two-dimensional (2D) electron gas in the hybrid structure turns into moving electron wires due to a very strong piezoelectric potential induced by a SAW. This effect has been demonstrated in the above-mentioned experiments [8] for the classical regime of the acoustoelectric (AE) interaction at room temperature. In the room-temperature electron system the dissipation of the SAW energy increases with increasing the sound intensity and approaches its maximum in the limit of the high amplitude of a SAW [8–10].

For low temperatures and a sufficiently strong PE potential of a SAW, the electron spectrum of wires can be quantized in the direction of the SAW momentum (Fig. 1b) [11–13]. For the first time the electron quantization effects in an acoustic wave have been discussed by Keldysh [11]. Our estimations show that the lateral quantization could be observed in low-temperature experiments on the recently fabricated hybrid structures.

Here we develop a quantum theory of the AE interaction in a 2D system in the strongly nonlinear regime when intense SAW's split a 2D electron system into moving quantum wires and dots. We model the AE interaction from first principles for the case of electron scattering by impurities and use time-dependent perturbation theory. In the quantum regime the SAW absorption due to electrons reflects the density of states in quantum wires. When a few quantum subbands are occupied the SAW energy dissipation comes mostly from the inter-subband transitions assisted by impurities. Furthermore, even in the strictly 1D case the SAW dissipation in quantum wires remains finite. The residual absorption of SAW in the 1D wires originates from the intra-subband transitions in the direction perpendicular to the SAW momentum. Our numerical results show that the residual SAW absorption in high-quality GaAs quantum wells is small enough and, so, the heating effect is weak in the quantum limit. In the case of two SAW's moving in the perpendicular directions, an electron system can be split into moving dots. In contrast to the case of wires, the SAW dissipation due to electron dots decreases and approaches zero in the quantum limit.

Many experimental papers report on interactions of SAW's with the quantum Hall effect systems and lateral nanostructures [14,15]. However, most of those studies relate to the linear regime of the AE interaction. A linear theory of the AE interaction in a 2D system and various nanostructures was developed in Refs. [16,17]. Also, theoretical aspects of single-electron transport through a quantum-point contact were discussed in Ref. [18].

The nonlinear AE interaction in the classical regime in bulk crystals was widely discussed

theoretically [10]. Recently a theory of the nonlinear AE effects has also been considered for the case of a classical 2D plasma in hybrid structures [9]. For the case of 3D plasma, the attenuation of sound in the presence of quantization in one direction was studied by Laikhtman and Pogorel'skii (Ref. [13]). They used the quasi-classical approach based on the Boltzmann equation and have predicted the quantum oscillations of the attenuation due to the density of states. Here we study the nonlinear quantum AE interactions for the case of a 2D system in the regimes of moving quantum wires and dots. Furthermore, we develop a quantitative theory based on the density-matrix motion equation. The quantum-mechanics treatment of this problem is necessary for the quantitative theory, which takes into account non-diagonal elements of the density matrix and the quantum dynamical screening of the impurity potential. In particular, the screening effect is important for the model of background Coulomb impurities. The calculations performed in the Coulomb-impurity model without the screening effect lead to the infinitely large sound attenuation. Basing on our numerical data we can conclude that the quantum attenuation regime is possible in high-mobility GaAs structures despite heating. It is in contrast to the AE interaction in the 3D plasma where the heating effect is predicted to be strong (Ref. [13]). In addition, we find that the sound dissipation in the case of driven quantum dots behaves differently compared to the nonlinear regimes in the 3D plasma and to the quantum wires.

II. GENERAL FORMALISM

The interaction between a SAW and a 2D electron system is characterized by the SAW energy absorbed in an electron system per unit time and aria

$$Q =< \mathbf{j}_s(\mathbf{r},t)\mathbf{E}_{SAW}(x,t) >_{\mathbf{r}}, \tag{1}$$

where $< ... >_{\mathbf{r}}$ means averaging over surface aria of a macroscopic sample. $\mathbf{r} = (x, y)$ is the in-plane coordinate and t is the time. The 2D electron current $\mathbf{j}_s$ in the plane of a quantum well is induced by the PE field of a SAW, $\mathbf{E}_{SAW}(x - c_s t)$. The Rayleigh SAW propagates in the x-direction with a velocity c_s and interacts with a 2D plasma (Fig. 1). In this case, the in-plain component of $\mathbf{E}_{SAW}$ is parallel to the x- axis. Eq. 1 can be used for a description of the SAW dissipation in the nonlinear regime in the limit of a weak AE coupling $K^2_{eff} \ll 1$ [9].

To find the electron current in the presence of the SAW piezoelectric field, we use the equation of motion for the one-particle density matrix $\hat{f}$ within the framework of the self-consistent field approximation [19],

$$\frac{\partial \hat{f}}{\partial t} + \frac{i}{\hbar}[\hat{H}, \hat{f}] = (\frac{\partial \hat{f}}{\partial t})_{Collisions}, \tag{2}$$

where $\hat{H}$ is the electron Hamiltonian.

The conventional approach to the equation (2) is based on the constant relaxation time τ and the assumption that the collision term in Eq. 2 is proportional to the divination from the local thermal equilibrium [19]. However, this approach is not effective in our case. By integrating Eq. 2 and the similar equation for the current we can show that the SAW-energy dissipation in the regime of well separated wires is $Q =< j_s E_{SAW} >_{\mathbf{r}} = m^* c_s^2 N_s/\tau$, where

m^* is the electron mass. Here $N_s =< n_s(x,t) >_x$ is the averaged 2D density and $n_s(\mathbf{r},t)$ is the local density. This result coincides with the Weinreich relation [20] obtained within the Drude model [9,10]. Thus, the absorption Q found in the simplified model does not exhibit any physical features of the lateral quantization.

To describe the AE interaction in the quantum wire regime we need to model scattering from the first principles. For low temperatures the main contribution to Q comes from the electron scattering by impurities [13,22]. So, we introduce the potential of randomly located impurities directly into the Hamiltonian in the right-hand side of Eq. 2. The Hamiltonian describing the in-plane single electron motion in the presence of SAW piezoelectric potential Φ_{SAW} is

$$\hat{H} = \frac{\hat{\mathbf{p}}^2}{2m} + e\Phi_{SAW}(x - c_s t) + U_{ind}(\mathbf{r},t) + U_{imp}(\mathbf{r}), \tag{3}$$

where $\hat{\mathbf{p}}$ is the in-plane momentum and e is the electron charge. $\Phi_{SAW}(x - c_s t) = \Phi^0_{SAW}\cos(kx - \omega t)$ is the piezoelectric potential and $\omega = c_s k$. U_{ind} is the potential induced by the electrons. $U_{imp}(\mathbf{R}) = \sum_i U_0(\mathbf{R} - \mathbf{R}_i)$, where $\mathbf{R} = (\mathbf{r}, z)$ is the 3D electron coordinate, and $U_0(\mathbf{R} - \mathbf{R}_i)$ is the potential of the i-impurity. Here the electron motion is 2D in the plane $z = 0$ whereas the impurity position R_i is a 3D vector. In a quantum well the electron motion in the z-direction is described by a localized wave function $\chi_0(z)$. For simplicity, we will neglect the width of the function $\chi_0(z)$ and consider the potential $U_{imp}(\mathbf{R})$ only in the plane $z = 0$. Also, we assume that electrons occupy only the ground 2D subband. To describe the SAW dissipation we intend to use the model of background Coulomb impurities with homogenous spatial distribution. In the following we will denote the average 3D density of impurities by N_t.

III. PERTURBATION THEORY

First we qualitatively analyze perturbation theory for the regime of wide wires where the quantization is negligible. The impurity potential is assumed to be weak perturbation. If the SAW intensity is sufficiently low a SAW slightly modulates a 2D plasma. In this linear regime [16], the sound absorption coefficient $\Gamma_0 = Q/I_{SAW} \propto \sigma_0 \propto \tau_{tr}$ when $\sigma_0 \to 0$. Here I_{SAW} is the SAW intensity. In the limit $U_0 \to 0$, $\tau_{tr} \to \infty$ and $Q \to \infty$. It shows that the simplest first-order perturbation theory is not valid. Indeed, it is known that the conductivity can be calculated as an infinite series of "ladder" diagrams [24]. The perturbation theory of Ref. [24] is based on the parameter $k_f l_e \gg 1$, where k_f and l_e are the Fermi wave vector and the electron mean free path, respectively. We see that the first diagram in terms of the impurity potential is not sufficient in the linear regime of the AE interaction. The situation in the nonlinear case is qualitatively different. For a high SAW intensity a 2D plasma forms well separated wires. When $I_{SAW} \to \infty$, the SAW dissipation due to classical wires becomes saturated and equal to $Q_{max} = m^* c_s^2 * N_s/\tau_{tr}$ [9,10,21]. One can see that $Q_{max} \propto 1/\tau_{tr} \to 0$ when $U_0 \to 0$. It means that we can calculate Q_{max} by using the first diagram in terms of the parameter U_0^2. In other words, in the case of wires the SAW potential confines strongly electrons and we can take into account the impurity scattering using simplest first-order perturbation theory. In the following we will use this fact to calculate the SAW absorption.

In the regime of wires, it is convenient to introduce the new moving coordinate $x' = x - c_s t$. In the moving coordinate system $\mathbf{r}' = (x', y)$, the strong SAW potential $e\Phi_{SAW}(x')$ is time-independent but the impurity potential $U_{imp}(\mathbf{r}', t)$ depends on the time. By changing $\mathbf{r} \to \mathbf{r}'$ we change $\hat{f}$ to $\hat{f}'$, where $\hat{f}'$ is the density matrix in the moving system of coordinates. Obviously, the motion equation (2) is conserved when $\mathbf{r} \to \mathbf{r}'$.

The quantum wire width l_0 is typically much less than the acoustic-wave length $\lambda \sim 1\ \mu m$ and, thus, the interaction between the quantum wires can be neglected. So, for convenience we will consider the density matrix for a single wire. In the moving coordinate system the electron current of a single wire contains only the random term $\delta\mathbf{j}_w$ which is induced by impurities. The dissipation is given by

$$Q = \frac{1}{\lambda} \int dx' < \delta\mathbf{j}_w(\mathbf{r}', t)\mathbf{E}_{imp}(\mathbf{r}', t) >_{\mathbf{R}_i}, \tag{4}$$

where $\mathbf{E}_{imp} = -\nabla_{\mathbf{r}'} U_{imp}(\mathbf{r}', t)/e$ is the random electric field of impurities. $< .. >_{\mathbf{R}_i}$ means averaging over random positions of impurities. Eqs. 1 and 4 are equivalent because the dissipation is independent of the coordinate system. The electron density and current in the static system can be written as $n_s(\mathbf{r}, t) = n_0(x - c_s t) + \delta n_1(\mathbf{r}, t)$ and $\mathbf{j}_s(\mathbf{r}, t) = \mathbf{j}_0(x - c_s t) + \delta\mathbf{j}_1(\mathbf{r}, t)$, respectively. Here δn_1 and $\delta\mathbf{j}_1$ are random terms. The regular contributions are connected by $\mathbf{j}_0 = e\mathbf{c}_s n_0(x - c_s t)$. The dissipation given by Eq. 1 is $Q = \int \mathbf{j}_0 \mathbf{E}_{SAW} dx$ because $< \delta\mathbf{j}_1(\mathbf{r}, t)\mathbf{E}_{SAW} >_{\mathbf{R}_i} = 0$. We can directly show that $\int \mathbf{j}_0 \mathbf{E}_{SAW} dx = \int < \delta\mathbf{j}_w \mathbf{E}_{imp} >_{\mathbf{R}_i} dx'$ if we multiply the equation of motion (2) by the current operator and then take the trace. Here we note that the electron density n_s and the currents relate to a single wire.

On the next step we consider linear response of a wide electron wire to the potential of "moving" impurities $U_{imp}(\mathbf{r}', t)$. In wide wires we can neglect the lateral quantization. In a small part of the electron wire, the electron plasma can be regarded as a homogeneous 2D Fermi gas. The linear response of a homogeneous 2D plasma to the potential $U_{imp}(\mathbf{r}', t)$ can be calculated from Eq. 2 [19]. The dissipation in the a small part of the channel near the point x'_0 is $\delta Q = \int_{x'_0}^{x'_0 + \delta x'} < \delta\mathbf{j}_w \mathbf{E}_{imp} >_{\mathbf{R}_i} dx'$. Then, using the dynamic 2D electron conductivity $\sigma_s(\mathbf{q}, \omega)$, we obtain $\delta Q = \delta x' n_s(x') c_s^2 m^*/\tau_{tr}$. After integration over all parts of the wire we again come to the above-mentioned equation for Q_{max}.

In the absence of impurities, the electron-electron scattering in the moving coordinate system results in thermal equilibrium. In this case the density matrix is equal to the Fermi distribution function $\hat{f}^0$ which depends on the electron temperature T_e. In the presence of weak impurity scattering the density matrix becomes equal to $\hat{f}' = \hat{f}^0 + \delta\hat{f}'$. The spectrum of quantum wires has the 1D subband structure: $E_{p_y,\alpha} = E_\alpha + p_y^2/2m^*$, where p_y and α are the y-component of the momentum and the subband index; $\alpha = 0, 1, 2, ...$. In the self-consistent field approximation, the electrons in an ideal wire move in the potential $e\Phi_{SAW}(x') + V_{ind}(x')$, where $V_{ind}(x')$ is the term induced by the Coulomb repulsion. The single-electron wave functions will be denoted as $\psi_\alpha(x')e^{ip_y y}$. Also, it is convenient to use the parabolic approximation for the SAW potential, $e\Phi_{SAW} = e\Phi^0_{SAW} + m^*\Omega_0^2 x'^2/2$, which is valid near the center of a wire. Here $\Omega_0 = k\sqrt{|e|\Phi^0_{SAW}/m^*}$.

In the coordinate system $(\mathbf{r}', t)$, the potential $U_{imp}(\mathbf{r}', t)$ at $z = 0$ plays the role of perturbation. By using a linear response theory [19] we find the Fourier transform of the charge density perturbation induced by the time-dependent impurity potential

$$\delta\rho(x',q_y,\omega)=e\sum_{\alpha,\beta}\psi_\alpha(x')\psi_\beta(x')<\psi_\alpha(x')|\tilde{U}_{imp}(x',q_y,\omega)|\psi_\beta(x')>\Pi_{\alpha,\beta}(\omega,q_y), \quad (5)$$

$$\Pi_{\alpha,\beta}(\omega,q_y)=\int\frac{dp_y}{\pi\hbar}\frac{f^0_{p_y,\alpha}-f^0_{p+q_y,\beta}}{\hbar\omega+E^0_{p_y,\alpha}-E^0_{p_y+q_y,\beta}+i0}$$

where q_y and ω appear after Fourier transformation in terms of y and t, respectively. Here we have neglected weak electron-electron scattering. $\tilde{U}_{imp}$ is the screened impurity potential at $z=0$.

Using Eqs. 4 and 5 we obtain

$$Q=\frac{1}{\lambda}\frac{N_t}{(2\pi)^2\hbar}\sum_{\alpha,\beta}\int dq_x dq_y D_{\alpha,\beta}(q_y,c_sq_x)<|U_0(q_x,q_y,Z_i)|^2>_{Z_i}* \quad (6)$$

$$|A_{\alpha,\beta}(q_x)|^2\int dp_y c_s q_x(f^0_{p_y,\alpha}-f^0_{p_y+q_y,\beta})\delta(\hbar c_s q_x+E^0_{p_y,\alpha}-E^0_{p_y+q_y,\beta}),$$

where N_t is the 3D impurity density. $A_{\alpha,\beta}(q_x)=\int dx\psi_\alpha(x)\psi_\beta(x)e^{iq_xx}$ and $D_{\alpha,\beta}(q_x,q_y,\omega)$ is the screening factor. The single-impurity potential is given by $U(q)=2\pi e^2/(\epsilon|q|)e^{-|Z_i||q|}$; $<|U_0|^2>_{Z_i}=(2\pi)^2e^4/(\epsilon^2|q|^3)$ and $\mathbf{q}=(q_x,q_y)$. The screening factor for the impurity potential in a quantum wire with many occupied subbands should be found from the system of linear equations [19]. In the simplest case of the lowest occupied 1D subband we obtain $D_{0,0}(q_y,\omega)=1/|\epsilon_{0,0}(q_y,\omega)|^2$, where $\epsilon_{0,0}(q_y,\omega)=1+V_{0,0}(q_y)\Pi_{0,0}(q_y,\omega)$ and $V_{0,0}$ is the matrix element of the Coulomb potential.

Equation 6 describes inter- and intra-subband transitions in a quantum wire induced by "moving" impurities. The momentum and energy transfers in these transitions are $\mathbf{q}=(q_x,q_y)$ and $\hbar\mathbf{qc_s}=\hbar c_sq_x$. In Fig. 1c we show electron transitions which contribute to Q. The difference between Eq.6 and the quasi-classical results of Ref. [13] is the screening factor $D_{\alpha,\beta}$ calculated from the quantum equations. In the case of a few occupied subbands, the screening factor has a complex structure.

Electron scattering by impurities also leads to the spatial shift of the electron distribution from the center of a quantum wire. This shift directly relates to the dissipation. Multiplying the equation of motion (2) by the current operator and then taking the trace, we can obtain the steady-state condition $Q/c_s=e(1/\lambda)\int<n_sE_{SAW}>_{\mathbf{R}_i}dx'$, where n_s relates to a single wire. Here the term $e\int<n_sE_{SAW}>_{\mathbf{R}_i}dx'$ is the averaged force acting on the electrons in the wire and $\lambda Q/c_s$ plays the role the friction force. The nonzero quantity $e\int<n_sE_{SAW}>_{\mathbf{R}_i}dx'=-m^*\Omega_0^2\int<x'n_s>_{\mathbf{R}_i}dx'$, i.e. it is proportional to the shift of the electron distribution from the wire center. We have directly calculated the shift $e\int<n_sE_{SAW}>_{\mathbf{R}_i}dx'$ using the second-order perturbation theory for the density matrix $\hat{f}'$. The obtained formula was consistent with the steady-state condition $Q/c_s=e(1/\lambda)\int<n_sE_{SAW}>_{\mathbf{R}_i}dx'$ and Eq. 6 for Q.

IV. NUMERICAL RESULTS FOR THE QUANTUM WIRE REGIME

In Figs. 2 and 3 we show the calculated SAW absorption as a function of the potential amplitude Φ^0_{SAW} for various temperatures. We choose the following parameters $\lambda=1\ \mu m$, $c_s=3.9*10^5\ cm/s$, $N_L=4*10^5\ cm^{-1}$, $N_s=N_L/\lambda=4*10^9\ cm^{-2}$, $N_t=4.1*10^{14}\ cm^{-3}$,

$m^* = 0.07m_0$, and $\epsilon = 12.5$. The Fermi energy in the 1D limit is $E_f^{1D} \simeq 2\ meV$. The parameter N_t is found from the low-temperature mobility of a 2D homogeneous gas μ_{2D}. For the mobility we take $\mu_{2D} = 3 * 10^6\ cm^2/Vs$ at the 2D density $3 * 10^{11}\ cm^{-2}$. μ_{2D} was calculated by using the Born approximation and involving the screened impurity potential [23].

Figure 2 shows the SAW absorption for the case of electron scattering by background impurities with a short-range potential. The 3D density and the potential of δ-impurities correspond to the 2D mobility $3 * 10^6\ cm^2/Vs$. To calculate μ_{2D} we take into account a finite width of a quantum well in the z-direction. In the case of δ-impurities we use the equation similar to Eq. 6 and involve a few lowest 1D subbands. To demonstrate a general behavior of $Q(\Phi_0^{SAW})$, we use the single-particle wave functions, neglecting self-consistent Coulomb effects. The function $Q(\Phi_{SAW}^0)$ reflects the density of states in a wire. For relatively small SAW potentials electrons occupy a few 1D subbands and the main contribution to Q comes from inter-subband transitions induced by impurities (Fig. 1c). The contribution of inter-subband transitions is responsible for the absorption in the quasi-classical and classical regimes. At $\Phi_{SAW}^0 \simeq 0.08\ V$ the Fermi level coincides with the bottom of the first exited subband $\alpha = 1$ which leads to a maximum in the function $Q(\Phi_{SAW}^0)$. When $\Phi_{SAW}^0 \to 0$, $Q \to Q_{max}$. For the small Φ_{SAW}^0, the features related to higher subbands are not seen because of finite temperature. For the high Φ_{SAW}^0 the electrons occupy only the ground subband. In the case of δ-impurities the dissipation Q is an increasing function of the potential amplitude in the limit of $\Phi_{SAW}^0 \to \infty$. In the latter case the SAW absorption occurs only due to intra-subband electron transitions (Fig. 1c).

Now we calculate the function $Q(\Phi_{SAW}^0)$ in the model of dynamically screened Coulomb impurities. We use the self-consistent field approximation and the variational method to find the wave functions $\psi_\alpha(x')$. In the Coulomb-impurity model, the SAW absorption strongly decreases with increasing the SAW potential amplitude Φ_{SAW}^0 (Fig. 3). At high Φ_{SAW}^0, the absorption Q becomes saturated. The residual absorption at $\Phi_{SAW}^0 \to \infty$ originates from scattering within the ground subband (Fig. 1c) and depends on the quality of a quantum well and on the electron density. Again at $\Phi_{SAW}^0 \simeq 0.2\ V$ we can see the characteristic maximum in the function $Q(\Phi_{SAW}^0)$ which reflects the electron occupation of the second subband. The maximum of $Q(\Phi_{SAW}^0)$ in Fig. 3 is shifted to higher potentials compared with the data of Fig. 2. The reason is the Coulomb interaction in a wire. Inter-subband transitions for small potentials Φ_{SAW}^0 result in the strong increase of Q.

The dynamic screening of Coulomb impurities plays the very important role. The dissipation Q calculated by Eq. 6 is non-convergent in the absence of the screening effect. Also, we find that the screening effect for intra-subband transitions is much stronger than that for inter-subband transitions. It leads to a strong increase of the absorption as the sound intensity decreases. Another effect of inter-particle interaction is that the energy spacing between 1D subbands becomes essentially less due to Coulomb repulsion in a wire [7]. The energy quantization in a wire is reduced by a factor of 2 after the inclusion of the self-consistent Coulomb effects. This effect is seen from the data of Fig. 2 and Fig. 3.

It is interesting to compare the quantum attenuation with that in the classical limit. At room temperature the absorption is increasing with Φ_{SAW} and becomes saturated for high sound intensities (insert of Fig. 3) [9,10]. The maximal absorption depends directly on the mobility: $Q_{max} = m^* c_s^2 * N_s/\tau_{tr}$. For the typical room-temperature parameters

$\mu = 5000\ cm^2/Vs$ and $N_s = 4 * 10^9\ cm^{-2}$ [8], we obtain $Q_{max} \simeq 2 * 10^5\ erg/s$ which is a few orders of magnitude larger than the calculated quantum-limit absorption.

Here we have calculated the SAW absorption assuming that the electronic temperature in a wire is independent of Φ^0_{SAW}. However, the electron temperature T_e can depend on Φ^0_{SAW} and differ from the lattice temperature T_l. The important factor is the phonon relaxation efficiency, which depends on a material. The heating effect can be analyzed by the energy balance equation $Q = P_{ph}$, where P_{ph} describes the efficiency of the electron energy relaxation due to the emission of acoustic phonons. Involving the deformation- potential and piezoelectric mechanisms we calculate the energy-loss rate $P_{ph}(T_l, T_e)$ for the driven electron wires in the $GaAs$-based quantum well [25]. Figs. 4 and 5 show the phonon energy-loss rate P_{ph} and the calculated heating temperature $\Delta T = T_e - T_l$ in the 1D limit for $\Phi^0_{SAW} = 2\ V$. Here we find the electron temperature from the equation $Q(T_e) = P_{ph}(T_l, T_e)$ for the case of Coulomb impurities (Fig. 5). One can see that the heating effect in the 1D quantum regime is small in high mobility systems (Fig. 5). At the same time, we find that at smaller SAW intensity, when the function Q rapidly increases, the heating effect in $GaAs$-wires is stronger and can destroy the quantum state. In particular, the maximum of the function $Q(\Phi^0_{SAW})$ for $\Phi^0_{SAW} \simeq 0.25\ V$ can vanish. For $\Phi^0_{SAW} \simeq 0.25\ V$ and $Q \simeq 10^4\ erg/(cm^2 s)$, the roughly estimated electron temperature in wires can be about 30 K.

As an example, we now discuss the solution of the balance equation $Q(T_e) = P_{ph}(T_l, T_e)$ for $T_l = 2\ K$ (Fig. 5). One can see that the crossing between the curves for Q and P_{ph} in Fig. 4 exists when $\mu > 0.8 * 10^6\ cm^2/Vs$ (Fig. 5). So, for given lattice temperature the solution of $Q(T_e) = P_{ph}(T_l, T_e)$ is not longer existing if the 2D mobility is low. We can speculate that, if $\mu < 0.8 * 10^6\ cm^2/Vs$, the SAW can heat the electron wire up to the temperature about 30 K. At $T_e \sim 30\ K$ the LO-phonon scattering starts to play the role [25]. Thus, the quantum regime can exist only in high-quality quantum wells. In addition, we note that the solutions of the balance equation shown in Figs. 4 and 5 are stable.

The predicted quantum effects can occur if the potential amplitude induced by a SAW is sufficiently high. For $N_L = 4 * 10^5\ cm^{-1}$, $T_e = 2\ K$, and $\lambda = 1\ \mu m$, the quantum 1D regime occurs when $\Phi^0_{SAW} > 1\ V$. The amplitudes Φ^0_{SAW} up to 2 V have been achieved in the experiments [8] on the hybrid structures with a closely-located top metallic gate for SAW's with $\lambda = 10\ \mu m$. Additional enhancement of quantum effects can be expected in hybrid structures involving even stronger piezoelectric materials (Potassium Niobate, $K^2_{eff} \sim 0.5$ [26]) and semiconductors with smaller effective masses ($InAs$, $m^* = 0.03 m_0$).

In most of experiments on SAW's [8,14] the measured quantity is the absorption coefficient $\Gamma = Q/I_{SAW}$, where I_{SAW} is the SAW intensity. The calculated SAW absorption becomes saturated at high sound intensity and thus Γ behaves as $1/I_{SAW}$ in the limit $I_{SAW} \to \infty$ [13,10]. To observe the quantum effects we suggest to measure directly the SAW absorption because it is not decreasing in the limit $I_{SAW} \to \infty$. In the experiments on hybrid structures the total measured absorption in a sample was about or more then $0.5\ erg/s$ [8]. In $GaAlAs$ systems, the observed absorption can be even less [14]. The total sound absorption in a sample with a surface aria S is given by $W = S * Q$. Using the data of Fig. 3 we obtain $W \sim erg/s$ for $T = 2\ K$, $\Phi^0_{SAW} > 1\ V$, and $S = 0.1 * 0.1\ cm^2$. Hence, the residual attenuation in the quantum 1D limit could be experimentally observed. In experiments, the electron plasma can be induced by the metal gate (Fig. 1) [8] or photogenerated [28]. Recently, the nonlinear AE interactions between SAW's and a photogenerated plasma

were observed in $GaAs$-based structures [28].

V. QUANTUM DOTS DRIVEN BY ACOUSTIC WAVES

In the presence of two SAW's with perpendicular wave vectors the electron motion can be quantized in two directions. Assume that SAW1 and SAW2 propagate in the x- and y-directions, respectively. Their potentials are $\Phi_{SAW1} = \Phi^0_{SAW1}\cos(kx - \omega t)$ and $\Phi_{SAW2} = \Phi^0_{SAW2}\cos(ky - \omega t)$. The total potential near its minimums can be approximated as $e\Phi_{SAW1} + e\Phi_{SAW2} \simeq e\Phi^0_{SAW1} + e\Phi^0_{SAW2} + (m^*/2)(\Omega_x^2 x'^2 + \Omega_y^2 y'^2)$, where the frequencies $\Omega_{x,y} = k\sqrt{|e|\Phi^0_{SAW1(2)}/m^*}$ depend on the intensities of the SAW's. In the moving coordinate system $(x', y') = (x - c_s t, y - c_s t)$, the electron spectrum is discrete and given by $E_{n,m} = \hbar\Omega_x(n + 1/2) + \hbar\Omega_y(m + 1/2)$. The corresponding wave function will be denoted as $\Psi_{n,m}(x', y') = \psi^x_n(x')\psi^y_m(y')$. In the following we will consider a single dot and, for simplicity, neglect the Coulomb interaction.

The electron current in a dot in the moving coordinate system can be calculated by using Eq. 2. The x'-component of the random electron current induced by impurities in the moving coordinate system is

$$\delta j_{ind,x'}(x', y', \omega) = -\frac{i\hbar e}{2m^*}\sum_{n,m,n_1,m_1}[\Psi_{n,m}(x', y')\frac{\partial\Psi_{n_1,m_1}(x', y')}{\partial x'} - \Psi_{n_1,m_1}(x', y')\frac{\partial\Psi_{n,m}(x', y')}{\partial x'}] \quad (7)$$
$$< \Psi_{n_1,m_1}|U_{imp}(x', y', \omega)|\Psi_{n,m} > \frac{f^0_{n,m} - f^0_{n_1,m_1}}{\hbar\omega + E_{n,m} - E_{n_1,m_1} + i0}.$$

The absorption of two SAW's by a single dot is given by

$$Q = \frac{1}{\lambda^2}\int dx'dy' < \delta\mathbf{j}_{ind} * \mathbf{E}_{imp} >_{\mathbf{R}_i} . \quad (8)$$

By using Eqs. 7 and 8 we obtain

$$Q = \frac{1}{\lambda^2}\frac{1}{4\pi}N_t 2\sum_{n,m,n_1,m_1}\int dq_x dq_y < |U_0(q)|^2 >_{Z_i} |A_{n,m,n_1,m_1}(\mathbf{q})|^2 \quad (9)$$
$$(c_s q_x + c_s q_y)(f^0_{n,m} - f^0_{n_1,m_1})\delta(\hbar c_s q_x + \hbar c_s q_y + E_{n,m} - E_{n_1,m_1}),$$

where $\mathbf{q} = (q_x, q_y)$ and $A_{n,m,n_1,m_1}(\mathbf{q}) = \int \Psi_{n,m}\Psi_{n_1,m_1}e^{i\mathbf{qr}}dxdy$. The factor 2 in Eq. 9 is due to the spin degeneracy.

For the case $\Phi^0_{SAW1} = \Phi^0_{SAW2} = \Phi^0_{SAW}$, the wave function $\Psi_{n,m} \propto e^{-r^2/2l_0}$, where $l_0 = \sqrt{\hbar/\Omega_0 m^*}$. In the limit $\Phi^0_{SAW} \to \infty$ and for low temperatures, the leading terms in Eq. 9 have the indexes $n - n_1 = \pm 1$ and $m = m_1$ or $m - m_1 = \pm 1$ and $n = n_1$. The asymptotic behavior of Q is

$$Q \propto e^{-\frac{\Omega_0^2 l_0^2}{2c_s^2}} = e^{-\frac{\hbar\Omega_0}{2m^* c_s^2}} = e^{-\sqrt{\frac{\Phi^0_{SAW}}{\Phi_s}}}, \quad (10)$$

where $\Phi_s = 4(m^* c_s^2)^2 * m^*/[e\hbar^2 k^2]$. We see that the absorption in the limit of the large SAW intensity decreases exponentially.

The absorption Q is a sum of two contributions Q_1 and Q_2 which relate to the SAW1 and the SAW2, respectively. In the general case $\Phi^0_{SAW1} \neq \Phi^0_{SAW2}$ and both Q_1 and Q_2 depend on Φ^0_{SAW1} and Φ^0_{SAW2}. It shows that there is a nonlinear quantum interaction between the SAW1 and SAW2. This interaction is seen from the expression for Q_1

$$Q_1 = \frac{1}{\lambda^2}\frac{1}{4\pi} N_t 2 \sum_{n,m,n_1,m_1} \int dq_x dq_y < |U_0(q)|^2 >_{Z_i} |A_{n,m,n_1,m_1}(\mathbf{q})|^2 \tag{11}$$
$$c_s q_x (f^0_{n,m} - f^0_{n_1,m_1}) \delta(\hbar c_s q_x + \hbar c_s q_y + E_{n,m} - E_{n_1,m_1}).$$

In this equation the energies $E_{n,m}$ depend on Φ^0_{SAW1} and Φ^0_{SAW2}. Physically, the first SAW interacts with the second because the latter changes the energy spectrum in dots. This interaction can be observed as giant quantum oscillations [27].

Recent experiments [28], which involved two SAW's propagating in the perpendicular directions, were performed using the pump-probe method. The first SAW had a high intensity and the second was a probing wave. These experiments demonstrated strongly nonlinear AE effects in the presence of photogenerated electrons and holes.

VI. INTENSE ACOUSTIC WAVES IN NANOSTRUCTURES

In this section, we briefly consider the nonlinear AE interaction in a nanostructure which includes an array of quantum wires. Electron quantum wires can be realized by etching a formerly uniform 2D system [7]. In our model a SAW propagates along the wire direction x (Fig.6). In the y-direction, the electron motion is finite due to the wire confinement. At high intensity, the SAW can induce moving electron dots. The electron potential near its minimum can be approximated by $(m^*/2)(\Omega^2_{SAW} x'^2 + \Omega^2_{wire} y^2)$, where Ω_{wire} describes the static confinement in a quantum wire in the y-direction and Ω_{SAW} is a function of the sound intensity. The SAW absorption is given by Eq. 11 with the corrections $\Omega_{SAW1} \to \Omega_{SAW}$, $\Omega_{SAW2} \to \Omega_{wire}$ and $\delta(\hbar c_s q_x + \hbar c_s q_y + E_{n,m} - E_{n_1,m_1}) \to \delta(\hbar c_s q_x + E_{n,m} - E_{n_1,m_1})$.

The calculated absorption of a SAW, Q, demonstrates giant quantum oscillations due to the discrete spectrum in 'moving' quantum dots (Fig. 6) . The minimums of Q occur due to the commensurability effect in the energy spectrum and correspond to the condition $s\Omega_{SAW} = s'\Omega_{wire}$, where s and s' are integers. For example, we consider the main minimum in $Q(I_{SAW})$ when $\Omega_{SAW} = \Omega_{wire} = 1\ meV$ ($s = s' = 1$). Under the condition $\Omega_{SAW} = \Omega_{wire}$, the spacing between energy levels is equal to $\Omega_{SAW} = 1\ meV$, and the absorption is dramatically suppressed. This is due to the exponential function (10). When Ω_{SAW} slightly differs from Ω_{wire}, the minimum spacing between energy levels becomes less and the absorption Q increases.

Experiments with SAW's propagating along quantum wires have been performed in Ref. [29]. In these experiments, SAW's drove photogenerated electrons and holes through the quantum wires fabricated on patterned interfaces.

VII. DISCUSSION

We see from our results that the acoustic absorption in an electron system in the quantum limit is very different to that in the classical case. In the classical plasma, $Q(\Phi^0_{SAW})$

approaches Q_{max} in the limit $\Phi^0_{SAW} \to \infty$ [8–10]. In the quantum case, the absorption $Q(\Phi^0_{SAW})$ first decreases with increasing Φ^0_{SAW} and then becomes saturated at the minimal quantum absorption which comes from residual scattering in the ground subband. When two intense SAW's form electron quantum dots, the absorption exponentially decreases. Thus, the dissipation of sound in a system with moving dots vanishes in the limit of the high acoustic intensity. This is due to the fully quantized spectrum in the dots.

In first principle approach the electron conductivity $\sigma_0 = e\mu n_s$ can be calculated as an infinite series of the "ladder" diagrams [24]. Another method to derive the formula for σ_0 is based on the so-called Landauer dipole [30]. In this method, the impurities induce the dipole moments in the moving coordinate system in which the electron plasma does not move. The resulting polarization should coincide with the electric field in a sample. The equality between the electric field and the impurity-induced polarization permits to find the conductivity. Here we use another argument based on dissipation. By using our arguments we can also obtain the formula for the conductivity. To do this, we calculate the dissipation in the moving coordinate system. Then, we compare the results for the moving and static coordinates.

In conclusion, we have developed a quantum theory of the nonlinear interaction between acoustic waves and a 2D electron system in the limit of the high acoustic intensity. The intense SAW creates electron quantum wires. The SAW absorption as a function of the sound intensity reflects the 1D density of states. In wide wires the SAW absorption originates from the inter-subband transitions. In the strictly 1D case there is still a residual SAW absorption, which comes from the intra-subband electron transitions. In the regime of quantum dots the SAW absorption approaches zero in the limit of high sound intensity. The modern hybrid structures can be a candidate to experimentally observe the described quantum nonlinear mechanisms of the acoustoelectric interaction.

We would like to thank A. Wixforth and J. P. Kotthaus for important motivating remarks, and B. Laikhtman, A. V. Chaplik, A. Mayer, and H.-J. Kutschera for helpful discussions. We gratefully acknowledge financial support by the Volkswagen-Foundation and by the Russian Foundation for Basic Research.

* E-mail: Govor@isp.nsc.ru

** E-mail: Kalam@isp.nsc.ru

REFERENCES

[1] B. J. van Wees et al., Phys. Rev. Lett. **60**, 848 (1988); D. A. Wharam et al., J. Phys. **C 21**, L209 (1988).

[2] R. Landauer, IBM J. Res. Dev. **1**, 223 (1957); R. Landauer, Phys. Lett. **85A**, 91 (1981); B.I. Halperin, Phys. Rev. B **25**, 2185 (1982); M. Büttiker, Phys. Rev. Lett. **57**, 1761 (1986).

[3] L.G.C. Rego and G. Kirczenow, Phys. Rev. Lett. **81**, 232 (1998); K. Schwab, E.A. Henriksen, J.M. Worlock, and M.L. Roukes, Nature, **404**, 974 (2000).

[4] J. M. Luttinger, J. Math. Phys. **4**, 1154 (1963); J. Voit, Rep. Prog. Phys. 58, 977 (1995); L. Calmels and A. Gold, Phys. Rev. B 56, 1762 (1997).

[5] A.O. Govorov and A.V. Chaplik, Zh. Eksp. Teor. Fiz. **99**, 1853 (1991) [Sov. Phys. JETP **72**, 1037-1046 (1991)].

[6] L. Jacak, P. Hawrylak, and A. Wojs, *Quantum dots* (Springer, Berlin, 1998); M. Grundmann, D. Bimberg, and N. N. Ledentsov, *Quantum Dot Heterostructures* (Wiley, New York, 1998).

[7] W. Hansen, M. Horst, J. P. Kotthaus, U. Merkt, Ch. Sikorski, and K. Ploog, Phys. Rev. Lett. **58**, 2586 (1987); E. Batke, D. Heitmann, and C. W. Tu, Phys. Rev. B **34**, 6951 (1986); T. P. Smith III et al., Phys. Rev. Lett. **59**, 2802 (1987); T. Egeler, G. Abstreiter, G. Weimann , T. Demel, D. Heitmann, P. Grambow , and W. Schlapp, Phys. Rev. Lett. **65**, 1804 (1987); A. R. Goni, A. Pinczuk, J. S. Weiner, B. S. Dennis, L. N. Pfeiffer, and K. W. West, Phys. Rev. Lett. **70**, 1151 (1993); H. Drexler et al., Phys. Rev. B **49**, 14074 (1994).

[8] M. Rotter, A. V. Kalameitsev, A. O. Govorov, W. Ruile, and A. Wixforth, Phys. Rev. Lett. **82**, 2171 (1999); M. Rotter, A. Wixforth, A. O. Govorov, W. Ruile, D. Bernklau, and H. Riechert, Appl. Phys. Lett. **75**, 965 (1999).

[9] A.O. Govorov et al., Phys. Rev. **B 62**, 2659 (2000).

[10] P.K. Tien, Phys. Rev. **171**, 970 (1968); V.L. Gurevich and B.D. Laikhtman, Zh. Eksp. Teor. Fiz. **46**, 598 (1964) [Sov. Phys. JETP **19**, 407 (1964)]; Yu.V. Gulyaev, Fiz. Tverd. Tela **12**, 415 (1970) [Sov. Phys. - Solid State, **12**, 328 (1970)].

[11] L.V. Keldysh, Fiz. Tverd. Tela **4**, 1015 (1962) [Sov. Phys. - Solid State].

[12] V.V. Popov and A.V. Chaplik, Zh. Eksp. Teor. Fiz. **73**, 1009 (1977) [Sov. Phys. JETP].

[13] B.D. Laikhtman and Yu.V. Pogorel'skii, Zh. Eksp. Teor. Fiz. **75**, 1892 (1978) [Sov. Phys. JETP, 8, 953 (1978)].

[14] A. Wixforth et al., Phys. Rev. **B40**, 7874 (1989); R.L. Willett et al., Phys. Rev. Lett. **71**, 3846 (1993); I.L. Drichko et al., Fiz. Tekh. Poluprovodn. **31**, 451 (1997) [Sov. Phys. Semiconductors **31**, 451 (1997)].

[15] V.I. Talyanskii et al., Phys. Rev. **B56**, 15180 (1997); J.M. Shilton et al., Phys. Rev. **B51**, 14770 (1995).

[16] K.A. Ingebrigtsen, J. Appl. Phys. **41**, 454 (1970); A.V. Chaplik, Pis. Zh. Tekh. Fiz. **10**, 1385 (1984) [Sov. Tech. Phys. Lett. **10**, 584 (1984)].

[17] V.L. Gurevich, V.B. Pevzner, and G.J. Iafrate, Phys. Rev. Lett. **77**, 3881 (1996); A.D. Mirlin and P. Wölfle, *ibid* **78**, 3717 (1997); Y. Levinson et al., Phys. Rev. **B 58**, 7113 (1998); C. Eckl, Yu.A. Kosevich, and A.P. Mayer, Phys. Rev. **B 61**, XXX (2000).

[18] G.R. Aizin, G. Gumbs, and M. Pepper, Phys. Rev. **B 58**, 10 589 (1998).

[19] M.P. Greene et al., Phys. Rev. **177**, 1019 (1969); K.S. Yu and J.J. Quinn, *ibid*, **B 27**, 1184 (1983).
[20] G. Weinreich, Phys. Rev. **107**, 317 (1957).
[21] The formula for Q_{max} can easily be obtained using the hydrodynamic equations. Within the Drude model, the friction force acting on an electron is equal to $f_{fr} = -v(r,t)m^*/\tau_{tr}$, where $v(r,t)$ is the local velocity in a 2D plasma. The SAW dissipation is $Q_{max} = - < f_{fr} v n_s >$. It follows from the conservation of charge that in the regime of separated wires $v(x,t) = c_s$ and so $Q_{max} = m^* c_s^2 * N_s/\tau_{tr}$.
[22] At low temperatures electrons driven by a SAW can not emit bulk acoustic phonons because $c_s < c_{l,t}$, where $c_{l,t}$ are the bulk phonon velocities. Thus, the phonon contribution to Q can be neglected.
[23] J.H. Davies, *The Physics of Low-Dimensional Semiconductors* (Cambridge, University-Press, UK, 1998).
[24] A.A. Abrikosov, L.P. Gorkov, and I.E. Dzyaloshinskii, *Methods of Quantum Field Theory in Statistical Physics* (Prentice-Hall, Englewood Cliffs, NJ, 1963).
[25] U. Bockelmann and G. Bastard, Phys. Rev. **B 42**, 8947 (1990); C. Kurdak et al., Appl. Phys. Lett. **67**, 386 (1995).
[26] M. Zgonik et al., J. Appl. Phys. **74**, 1287 (1993).
[27] A.O. Govorov, A.V. Kalameitsev, V.M. Kovalev, H.-J. Kutschera, and A. Wixforth, Phys. Rev. Lett. 87, 226803 (2001).
[28] C. Rocke, A.O. Govorov, A. Wixforth, G. Böhm, and G. Weimann, Phys. Rev. **B 57**, R6850 (1998); M. Streibl, A. Wixforth, J.P. Kotthaus, A.O. Govorov, C. Kadow, and A.C. Gossard, Appl. Phys. Lett. 75, 4139 (1999).
[29] P. Santos et al., Proceedings of ICPS-2002, Edinburgh.
[30] R. Landauer, Z. Phys. **B 21**, 247 (1975); W. Zwerger et al., Phys. Rev. **B 43**, 6434 (1991).

Figure Captions

Fig. 1
a) The cross section of a hybrid semiconductor-piezoelectric structure. The electron density in a quantum well depends on the transport gate voltage V_t. A SAW propagates near the surface and interacts with the 2D plasma in a quantum well.
b) The moving piezoelectric potential of a SAW and the energy structure of moving quantum wires.
c) Intra-subband transitions in the 1D limit when electrons occupy only the ground subband. The second diagram shows the inter-subband transitions when electrons occupy the two lowest subbands.

Fig. 2 Calculated SAW absorption as a function of the potential amplitude Φ^0_{SAW} for various temperatures for the case of δ-impurities. $\lambda = 1\ \mu m$, $N_L = 4 * 10^5\ cm^{-1}$, $N_s = 4{*}10^9\ cm^{-2}$, and $N_t = 4.1{*}10^{14}\ cm^{-3}$. The low-temperature mobility in a homogeneous 2D gas with $N_s = 3 * 10^{11}\ cm^{-2}$ is equal to $3 * 10^6\ cm^2/Vs$.

Fig. 3 Calculated SAW absorption as a function of the potential amplitude Φ^0_{SAW} for various temperatures for the case of background Coulomb impurities which are dynamically screened by electrons. The parameters are similar to those of Fig. 2. Insert: the SAW absorption $Q_{class}(\Phi^0_{SAW})$ for the case of a classical electron system in a quantum well at room temperature.

Fig. 4 The energy-loss rate due to acoustic phonon emission in quantum wires formed by a SAW as a function of the electron temperature T_e for various lattice temperatures T_l (solid curves). The dashed curves show the SAW dissipation $Q(T_e)$ in the quantum regime for the case of Coulomb impurities. The dashed curves 1 and 2 relate to $\mu_{2D} = 1$ and $3 * 10^6\ cm^2/Vs$, respectively. The corresponding impurity densities are $N_t = 12.3$ and $4.1 * 10^{14}\ cm^{-3}$. The 2D mobility is calculated for $N_s = 3 * 10^{11}\ cm^{-2}$. The crossing points give the electron temperature in a wire. $\Phi^0_{SAW} = 2\ V$.

Fig. 5 The heating temperature $\Delta T = T_e - T_l$ in a wire as a function of the mobility μ_{2D} for the system with Coulomb impurities; the lattice temperature $T_l = 2\ K$; $\Phi^0_{SAW} = 2\ V$. $\lambda = 1\ \mu m$ and $N_L = 4 * 10^5\ cm^{-1}$. The 2D mobility is calculated for $N_s = 3 * 10^{11}\ cm^{-2}$.

Fig. 6 Calculated SAW absorption as a function of the quantization $\hbar\Omega^0_{SAW}$ in the system with etched quantum wires; the energy $\hbar\Omega_{wire}$ describes the static quantization in the potential of wires. Insert: Sketch of the system with etched quantum wires and a SAW. The velocity of dots is $(c_s, 0)$.

FIGURES

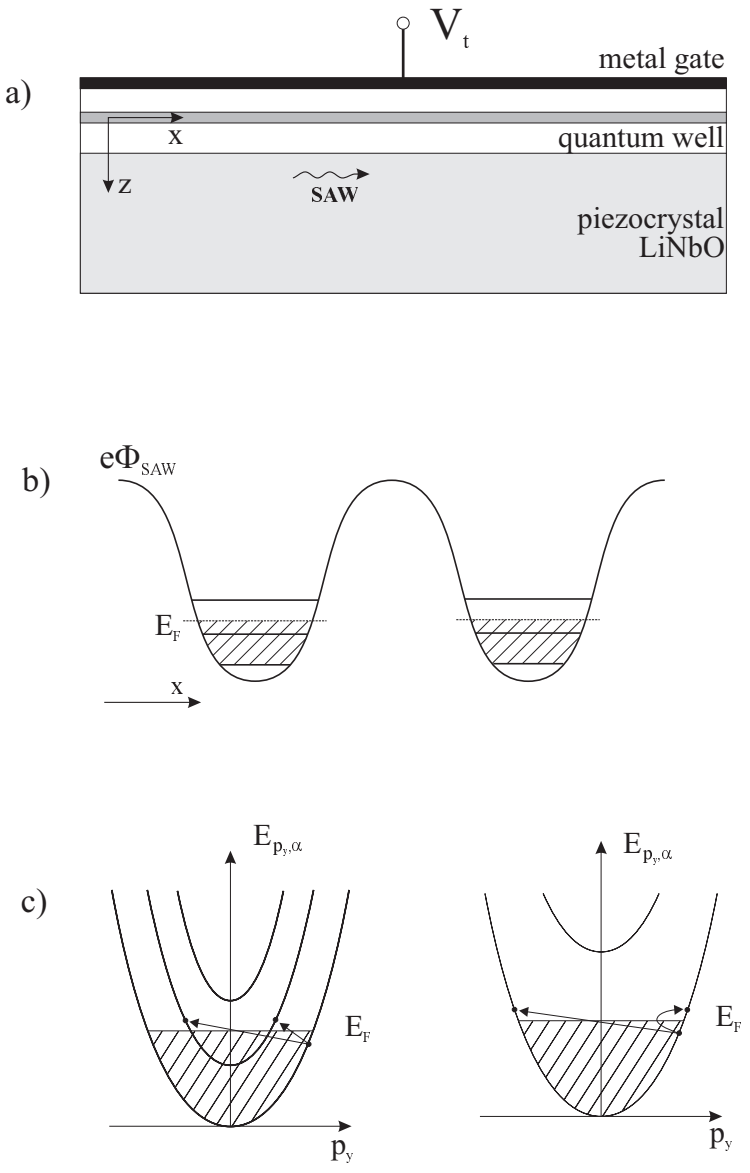

Fig. 1

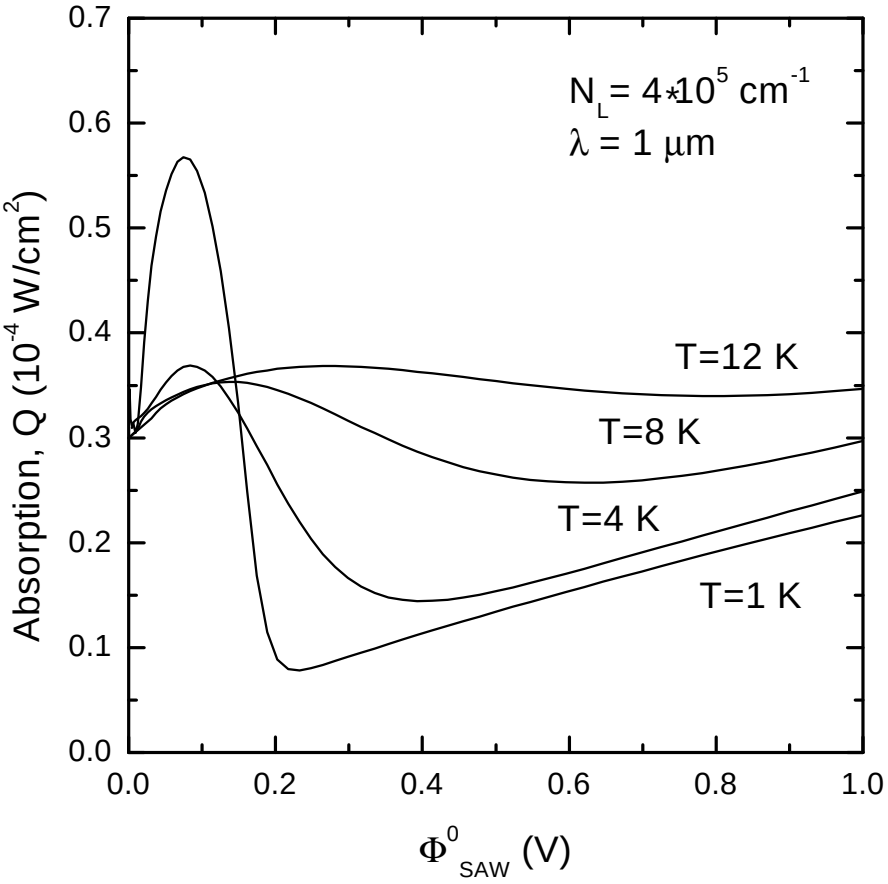
0.7
0.6
0.5
0.4
0.3
0.2
0.1
0.0
0.0
0.2
0.4
0.6
0.8
1.0
Absorption, Q (10^{-4} W/cm^2)
Φ^0_{SAW} (V)
$N_L = 4*10^5$ cm^{-1}
λ = 1 μm
T=12 K
T=8 K
T=4 K
T=1 K

Fig. 2

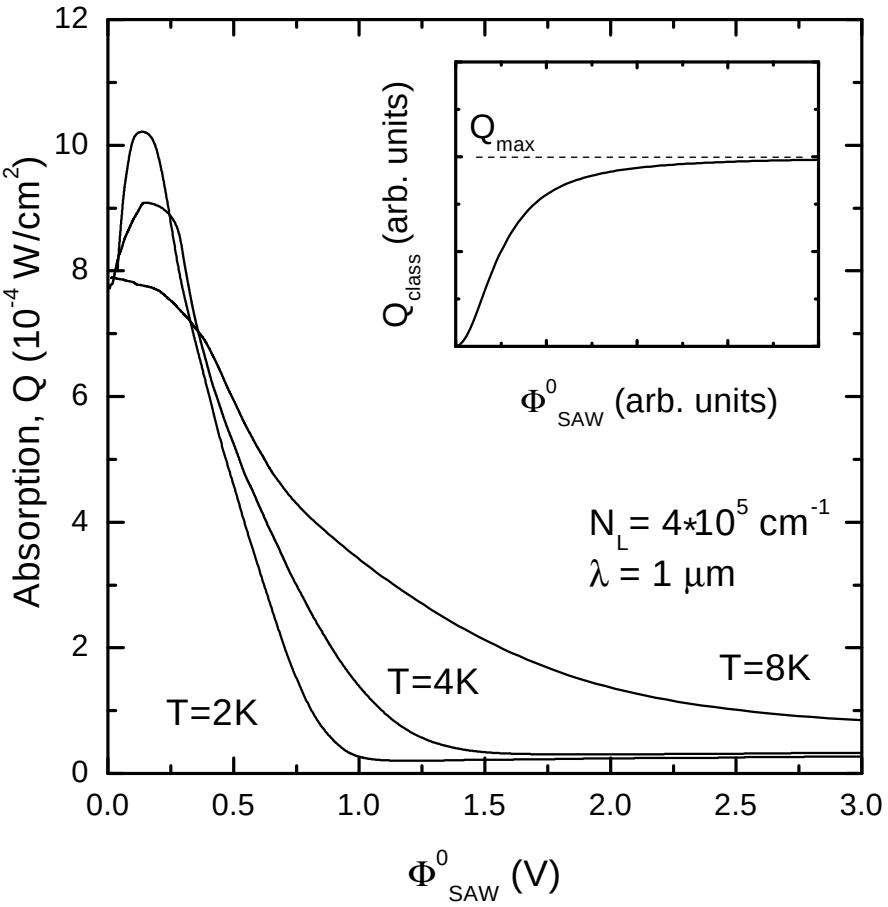
Absorption, Q (10^{-4} W/cm^2)
Φ^0_{SAW} (V)
Q_{class} (arb. units)
Q_{max}
Φ^0_{SAW} (arb. units)
$N_L = 4*10^5$ cm^{-1}
λ = 1 μm
T=2K
T=4K
T=8K

Fig. 3

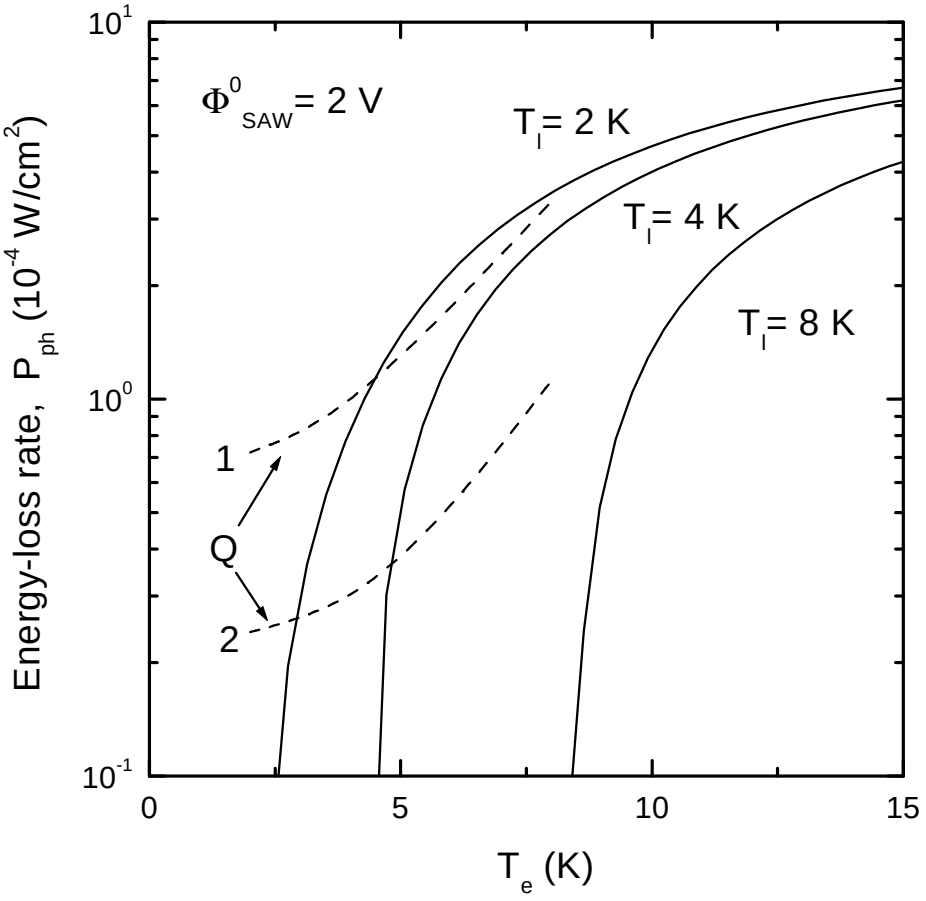
10^1
10^0
10^{-1}
Φ^0_{SAW}= 2 V
T_l= 2 K
T_l= 4 K
T_l= 8 K
1
Q
2
Energy-loss rate, P_{ph} (10^{-4} W/cm^2)
0
5
10
15
T_e (K)

Fig. 4

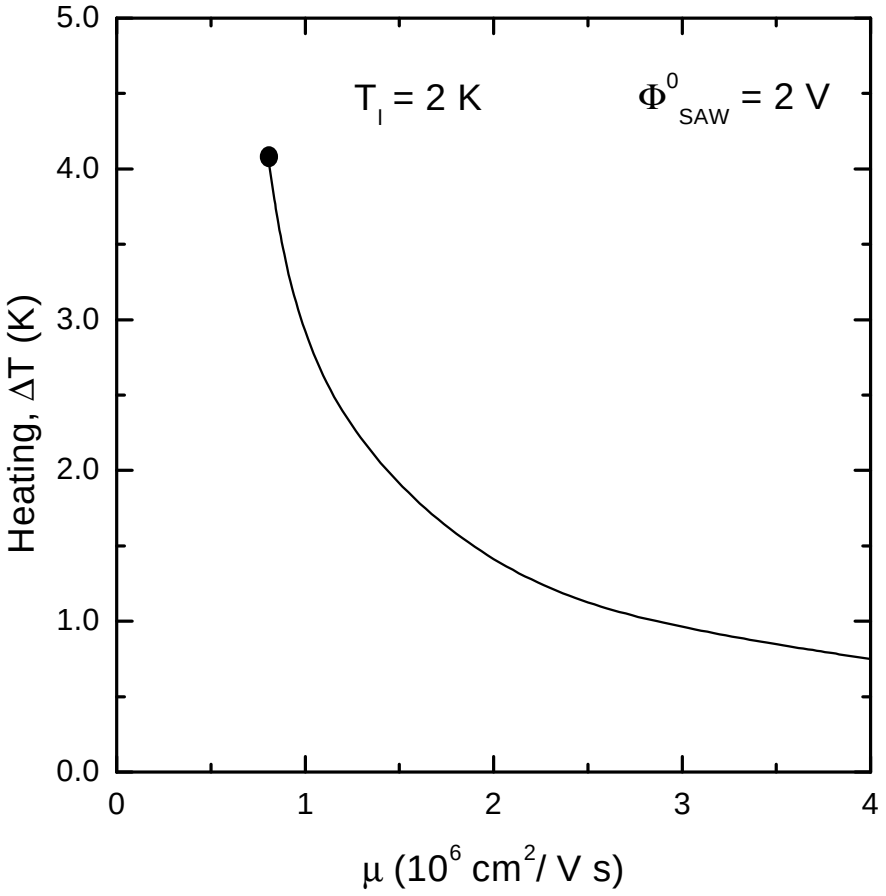

Fig. 5

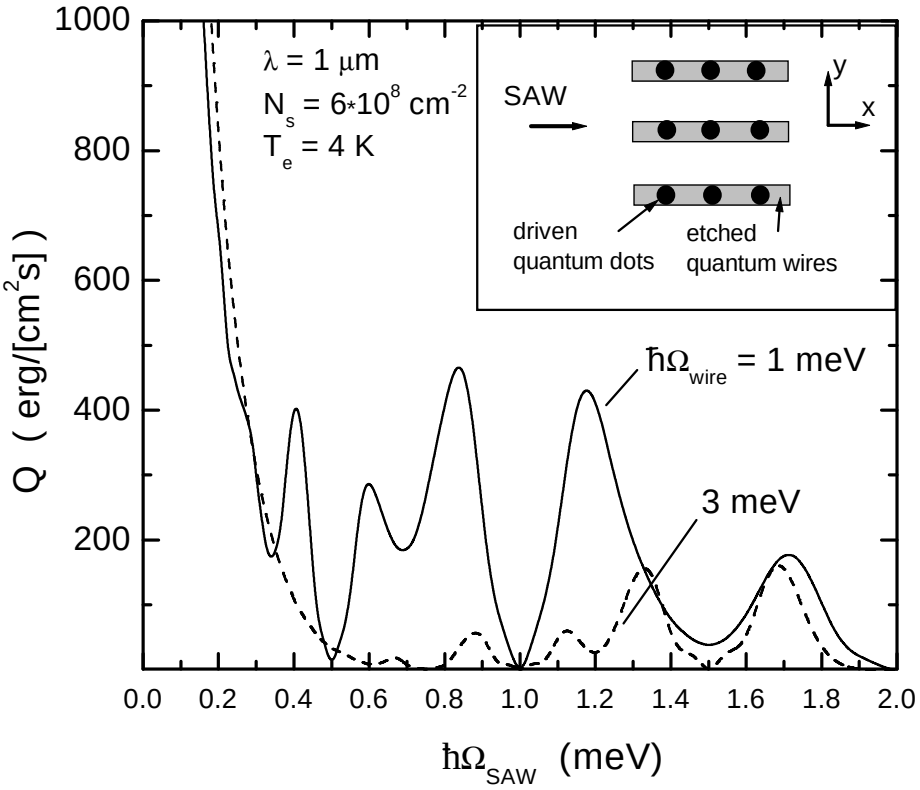
λ = 1 μm
N_s = 6*10^8 cm^-2
T_e = 4 K
SAW
y
x
driven
quantum dots
etched
quantum wires
ħΩ_wire = 1 meV
3 meV
Q (erg/[cm^2s])
ħΩ_SAW (meV)
1000
800
600
400
200
0.0
0.2
0.4
0.6
0.8
1.0
1.2
1.4
1.6
1.8
2.0

Fig. 6